BULLETIN OF THE POLISH ACADEMY OF SCIENCES
TECHNICAL SCIENCES, Vol. 64, No. 1, 2016
DOI: 10.1515/bpasts-2016-0011

Sequential separation of twin pregnancy electrocardiograms

M. KOTAS[1*], J.M. LESKI[1], and J. WROBEL[2]

[1] Institute of Electronics, Silesian University of Technology, 16 Akademicka St., 44-100 Gliwice, Poland
[2] Department of Computer Medical Systems, Institute of Medical Technology and Equipment, 118 Roosevelt St., 41-800 Zabrze, Poland

Abstract. We propose to tackle the problem of maternal abdominal electric signals decomposition with a combined application of independent component analysis and projective or adaptive filtering. The developed method is employed to process the four-channel abdominal signals recorded during twin pregnancy. These signals are complicated mixtures of the maternal ECG, the ECGs of the fetal twins and noise of various origin. Although the independent component analysis cannot separate the respective signals, the proposed combination of the methods deals with this task successfully. A simulation experiment confirms high efficiency of this approach.

Key words: fetal ECG, twin pregnancy, ECG signals decomposition, blind source separation, independent component analysis, source subspaces, projective filtering, adaptive filtering.

1. Introduction

The fetal electrocardiogram (FECG) is a source of the complex diagnostic information which can be analyzed by obstetricians for the assessment of the fetal well-being [1]. Numerous attempts have been made to develop effective methods of the FECG signals recording and analysis. The non-invasive approach, we focus on in this paper, is based on the signals recorded from the maternal abdominal wall. Such signals contain not only the fetal ECG but primarily the maternal electrocardiogram (MECG) and various types of noise (e.g. maternal muscles activity or artifacts resulting from fetal movements). Since in most cases the maternal electrocardiogram amplitude significantly exceeds that of the fetal ECG, an essential problem is the efficient suppression of this prevailing component [2].

Two most important approaches to cope with the problem can be distinguished. The first one is based on the analysis of single-channel signals. It exploits the approximate repeatability of the ECG beats to achieve the goal of the abdominal signals separation. Construction of the MECG beat template and subtraction of this template from the analyzed signal in the places where individual beats occur is a simple, yet effective solution of the problem [3]. The second approach is based on the analysis of multi-channel signals. In [4] application of adaptive filtering was described, with a few thoracic signals at the reference inputs, combined to cancel the maternal ECG in the abdominal signals. In [5] the weighted addition of four signals from the abdominal wall was performed to suppress the maternal ECG. A set of important techniques was based on the application of singular value decomposition to the separation of the maternal and the fetal source signals [6]. Application of independent component analysis (ICA), exploiting not only the second (as in [6]) but also higher order statistical conditions of independence, allowed to achieve a great progress in the accomplishment of the separation task [7, 8]. Both mentioned methods involve the redundancy of the multichannel ECG recordings. Therefore they require at least three or four channels to achieve the goal of the fetal ECG extraction. In cases of twin pregnancy, however, even larger number of channels does not guarantee the methods success in separating the ECG signals of the twins.

In this work we propose a different solution of the problem. A combination of approaches typical for the multichannel and the single-channel techniques makes possible exploiting both types of ECG signals redundancy. The independent component analysis performs the spatial separation of the abdominal signals; a single-channel approach based on projective filtering of the time-aligned ECG beats [9] or adaptive impulse correlated filtering [10] is employed to improve the results of the separation. The developed method operates repeatedly, and each time it separates one source signal only.

The rest of the paper is organized as follows: Sec. 2 describes the method proposed, in Sec. 3 its operation is illustrated and investigated, and in Sec. 4 we formulate the final conclusions.

2. Methods

2.1. Projective filtering of time-aligned beats (PFTAB). In the preprocessing phase of projective filtering, we perform detection and cross-correlation function based synchronization of the QRS complexes. This way a set of fiducial marks $\{r_k | k = 1, 2, \ldots, K+1\}$, corresponding to the same position within the respective $K+1$ QRS complexes, is created. Once the fiducial marks are established, the intrinsic operations of the method begin. They are as follows.

1. Reconstruction of the state-space representation [11] of the observed noisy signal by application of the Takens embedding operation [12]; a point in the reconstructed state-space is a vector:

*e-mail: mkotas@polsl.pl

$$\mathbf{x}^{(n)} = [x(n), x(n+\tau), \ldots, x(n+(m-1)\tau)]^\top, \quad (1)$$

where $x(n)$ is the processed signal, τ is the time lag ($\tau = 1$ is used in this application) and m is the embedding dimension.

2. The learning phase of the method: application of principal component analysis (PCA [13]) to the construction of signal subspaces for each position within an ECG beat.
3. The processing phase: correction of each individual point $\mathbf{x}^{(n)}$, by its projection into the corresponding signal subspace, and finally conversion of the corrected points back into one-dimensional signal.

In order to facilitate construction of local signal subspaces (LSS) for all positions within a beat, the beats are stored in an auxiliary matrix $\mathbf{T}$. We assume that a beat begins b samples before its fiducial mark and ends $b+1$ samples before the fiducial mark of the next beat (in the experiments that are presented, we used b corresponding to 150 ms). Each beat occupies one column of $\mathbf{T} = [\mathbf{t}_1, \mathbf{t}_2, \ldots, \mathbf{t}_K]$. The number of rows depends on the length $RR_{\max}$ of the longest beat. It must be large enough to allow construction of a signal subspace for $j = RR_{\max}$. Thus, we set $I = RR_{\max} + (m-1)$, and all the beats in $\mathbf{T}$ are extended to this length; we apply the method of zero order extension that extends a beat by repeating its last sample.

Storing the beats in matrix $\mathbf{T}$ enables easy determination of so-called neighborhoods corresponding to the respective positions within a beat. To this end for each j ($1 \le j \le RR_{\max}$) we first select a submatrix of $\mathbf{T}$ ($\mathbf{T}^{(j)} = [\mathbf{t}_1^{(j)}, \mathbf{t}_2^{(j)}, \ldots, \mathbf{t}_K^{(j)}]$; $t_{i,k}^{(j)} = t_{j+i-1,k}$) containing the vectors that correspond to the synchronized trajectory points. Then we form neighborhood $\Gamma^{(j)}$ corresponding to the j-th position within a beat by rejection of the assumed fraction c_ρ of the most distant points (those whose Euclidean distance to the neighborhood center is largest; $c_\rho = 0.1$ was used during the experiments that are presented).

After determination of a local neighborhood we proceed with construction of a local signal subspace. First, a local mean $\overline{\mathbf{t}}^{(j)}$ is computed and then the covariance matrix of the deviations from the mean

$$\mathbf{C}^{(j)} = \frac{1}{\operatorname{card}\left(\Gamma^{(j)}\right)} \sum_{k \in \Gamma^{(j)}} \left(\mathbf{t}_k^{(j)} - \overline{\mathbf{t}}^{(j)}\right)\left(\mathbf{t}_k^{(j)} - \overline{\mathbf{t}}^{(j)}\right)^\top, \quad (2)$$

where $\operatorname{card}(\cdot)$ is the cardinality of a set.

Then we perform eigendecomposition of the covariance matrix

$$\mathbf{C}^{(j)} = \mathbf{E}^{(j)} \Delta^{(j)} \mathbf{E}^{(j)\top}, \quad (3)$$

where $\mathbf{E}^{(j)} = \left[\mathbf{e}_1^{(j)}, \cdots, \mathbf{e}_m^{(j)}\right]$, $\Delta^{(j)} = \operatorname{diag}\left(\delta_1^{(j)}, \cdots, \delta_m^{(j)}\right)$.

Eigenvectors $\mathbf{e}_i^{(j)}$ of the j-th covariance matrix are the principal axes [13] (principal components directions) of the neighborhood points deviations from the mean. The corresponding eigenvalues $\delta_i^{(j)}$ are equal to the total energy of the deviations in the respective directions. The eigenvectors $\mathbf{e}_i^{(j)}$ are sorted with respect to the corresponding eigenvalues so that $\delta_1^{(j)} \ge \delta_2^{(j)} \ge \ldots \ge \delta_m^{(j)}$. The signal subspaces are composed of the first Q ($Q < m$) principal axes

$$\mathbf{E}_Q^{(j)} = \left[\mathbf{e}_1^{(j)}, \cdots, \mathbf{e}_Q^{(j)}\right]. \quad (4)$$

Construction of signal subspaces for all positions within a beat ends the learning phase of the method.

In the processing phase, we first determine a position j within a beat, the point under correction belongs to

$$\underset{r_k - b \le n < r_{k+1} - b}{\forall} j(n) = \begin{cases} n - r_k + b + 1, & n - r_k + b < RR_{\max} \\ RR_{\max}, & \text{otherwise} \end{cases}. \quad (5)$$

and then we project the point into the corresponding signal subspace

$$\mathbf{x}'^{(n)} = \overline{\mathbf{t}}^{(j(n))} + \mathbf{E}_Q^{(j(n))} \mathbf{E}_Q^{(j(n))\top} \left(\mathbf{x}^{(n)} - \overline{\mathbf{t}}^{(j(n))}\right). \quad (6)$$

The n-th sample of the processed signal occurs in m trajectory points, as the l-th entry $x_l^{(n-l+1)}$ of the vector $\mathbf{x}^{(n-l+1)}$. Averaging the results of the respective points projection leads to the following formula for the corrected signal sample

$$x'(n) = \frac{1}{m} \sum_{l=1}^{m} x_l'^{\,(n-l+1)}. \quad (7)$$

The method can be regarded as an extension of the popular method of time averaging [14, 15] but contrary to the averaging it preserves the variability of the ECG beats morphology. It can effectively be applied to suppress the muscular noise whose spectrum overlaps that of the desired ECG signal. Although in this application the further modifications of nonlinear projective filtering are more effective [16], PFTAB appeared more advantageous in extraction of FECG component from the single-channel signals recorded from the maternal abdominal wall [9]. In this application the method is used to enhance the maternal ECG (by suppressing the fetal ECG and noise) and later this component is subtracted from the original signal. This leads to maternal ECG suppression and fetal ECG extraction. In this application of PFTAB it was favorable to use higher dimensions of signal subspaces near the maternal QRS complexes (e.g. $Q = 2$) and lower in other parts of the processed signals ($Q = 1$ or $Q = 0$); such dimensions are denoted as $Q = 2|1$ and $Q = 2|0$, respectively. This way the complexes, which are the most variable part of the ECG beats, are reconstructed more precisely and then more effectively suppressed.

2.2. Blind source separation model. The model has widely been used in many applications [6–8,17–20]. It is based on the assumption that the signals from different leads are different linear combinations of the same source signals, independent from one another

$$\mathbf{x}(n) = \mathbf{A}\mathbf{z}(n) + \boldsymbol{\eta}(n), \quad (8)$$

where $\mathbf{x}(n) = [x_1(n), \cdots, x_K(n)]^\top$ denotes the observation vector in the measurement space (the measured signals vector), $\mathbf{z}(n) = [z_1(n), \cdots, z_K(n)]^\top$ is the source signals vector,

$\boldsymbol{\eta}(n) = [\eta_1(n), \cdots, \eta_K(n)]^\top$ – the vector of the noise components; $\mathbf{A}$ is the mixing (projecting) matrix, with the entry $a_{i,k}$ by which the k-th source signal is multiplied to form the i-th observation

$$x_i(n) \sum_{k=1}^{K} a_{i,k} z_k(n) + \eta_i(n), \qquad i = 1, \cdots, K. \tag{9}$$

For simplicity the same number of measured and source signals, equal to K, is assumed in the model.

Knowing the projecting matrix $\mathbf{A}$ and assuming that it can be inverted, we can calculate the separating matrix $\mathbf{B} = \mathbf{A}^{-1}$ and then decompose the measured signals as follows

$$\begin{aligned} \widehat{\mathbf{z}}(n) &= \mathbf{B}\mathbf{x}(n) = \mathbf{A}^{-1}\mathbf{A}\mathbf{z}(n) + \mathbf{A}^{-1}\boldsymbol{\eta}(n) \\ &= \mathbf{z}(n) + \mathbf{A}^{-1}\boldsymbol{\eta}(n). \end{aligned} \tag{10}$$

However, since $\mathbf{A}$ is usually unknown, we have to perform the "blind source separation", only on the basis of the source signals statistical independence.

To this end we applied the JADE (which stands for Joint Approximate Diagonalization of cumulant Eigenmatrices [21]) algorithm, exploiting the second order (covariance) and the fourth order (cumulants) conditions of the statistical independence. Applying JADE we obtain the estimates of the mixing ($\widehat{\mathbf{A}}$) and separating matrix ($\widehat{\mathbf{B}}$). They are determined with the assumption of the source signals spatial whiteness ($E\left[\mathbf{z}\mathbf{z}^\top\right] = \mathbf{1}$). This assumption is allowable because of the known ambiguity of model (8) in which we cannot evaluate the variances of the source signals (since multiplying a source signal $z_i(n)$ by a constant can be compensated by dividing the corresponding column $\widehat{\mathbf{a}}_i$ of the mixing matrix).

2.3. Assessment of ECG signals quality. The ECG signals characteristic feature is their approximate repeatability. This feature can be evaluated with the use of the autocorrelation function

$$R_{xx}(\tau) = E\left[x(n)x(n+\tau)\right]. \tag{11}$$

For strictly periodic signals, the function has a maximum for every multiple of the signal period. However, the length of the successive ECG cycles can differ. Moreover, the dominant ECG waves (the QRS complexes) have some parts of different polarization. These features can complicate evaluation of the signals periodicity. As far as the fetal ECG is regarded, some difficulties can also be caused by a considerable noise energy (if compared to the energy of the desired FECG). To make the use of the autocorrelation function for ECG signals quality evaluation more effective, we developed the following approach [22]:

- First the operation enhancing the QRS complexes is determined (to this end we applied the classical detection function based on linear filtering, squaring and moving window integration [23]).
- Then N_i equidistant signal parts, located in a time-window of the assumed length, are selected.
- On the basis of the windowed detection function, the autocorrelation function is computed.
- For each time-window (see Fig. 1), we calculate the local quality index QI_i by searching for the largest value (h_1) of the autocorrelation function in the allowable range of the delay variable τ and then finding the smallest value (h_2) preceding h_1: $QI_i = h_1/h_2$ ($h_2 > 0$ because the detection function used is always nonnegative).
- Finally, the median value of the obtained indices is calculated

$$QI = \text{median}\{QI_i \mid i = 1, 2, \cdots, N_i\}. \tag{12}$$

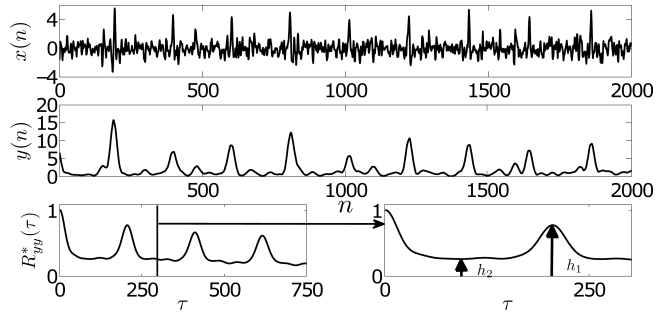

Fig. 1. Determination of the ECG signals quality index. From the top: the analyzed signal ($x(n)$), the calculated detection function ($y(n)$) and the normalized autocorrelation function ($R^*_{yy}(\tau) = R_{yy}(\tau)/R_{yy}(0)$). For the presented i-th signal segment, the index (QI_i) is equal to h_1/h_2

The larger value of the index means that one periodic component dominates in the signal. In such a case, we can conclude that the level of noise is low and efficient suppression of other periodic ECG components was achieved. For a very poor separation, the index value decreases to 1.

2.4. Sequential determination of source subspaces. Although estimation of source signals is based on the assumption of their statistical independence, the common origin of some estimates does not confirm this assumption. Therefore, in the papers [7,24,25], the concept of independent source subspaces determination was introduced. The estimates of source signals are grouped with respect to their origin (the maternal or fetal hearts) and they compose the subspaces that can be employed for reconstruction of the corresponding components of the measured signals. If we denote as $\mathcal{F}$ the set containing the numbers of the source signals that belong to the same subspace (for simplicity such a set is called as a subspace itself), the operation can be expressed in the following way

$$_{\mathcal{F}}x_i(n) = \sum_{k \in \mathcal{F}} \widehat{a}_{i,k}\widehat{z}_k(n), \qquad i = 1, \cdots, K, \tag{13}$$

where $\widehat{z}_k(n)$ is the k-th estimated source signal, $\widehat{a}_{i,k}$ is the entry of the mixing matrix, $_{\mathcal{F}}x_i(n)$ is the component of the i-th measured signal, reconstructed on the basis of subspace $\mathcal{F}$.

When the number of source signals is larger than the number of the measured ones, independent component analysis can not assure their perfect separation. To accomplish this task in such conditions, we developed the method of sequential determination of source subspaces (SDSS) [22]. Its operation

can be summarized as follows. We perform independent component analysis many times: each time we select the source signal of the best quality, we enhance it with the use of some filter, and then we reconstruct and subtract the corresponding components of the measured signals. In the description that follows, the measured signals and the signals obtained after the aforementioned subtraction are called as the basic signals. The initial vector of the basic signals is denoted as $\mathbf{x}^{[0]}(n) = \mathbf{x}(n)$.

`SDSS algorithm`

1. The iteration counter ℓ is preset: $\ell = 1$.
2. For the basic signals obtained after accomplishment of the previous iteration, the JADE algorithm is applied to determine the estimates $\widehat{\mathbf{B}}^{[\ell]}$ and $\widehat{\mathbf{A}}^{[\ell]}$ of the separating and mixing matrices; then the source signals estimation is performed $\widehat{\mathbf{z}}^{[\ell]}(n) = \widehat{\mathbf{B}}^{[\ell]}\mathbf{x}^{[\ell-1]}(n)$.
3. For each of the K determined estimates of the source signals, contained in vector $\widehat{\mathbf{z}}^{[\ell]}(n)$, the quality index defined by (12) is calculated.
4. We find the number ($v^{[\ell]}$) of the source signal estimate for which the largest value of the index ($QI^{[\ell]}_{\max}$) has been obtained in the current iteration.
5. The condition of the iterations termination: $QI^{[\ell]}_{\max} < QI_\theta$ is checked (QI_θ is the assumed minimal value of the quality index). When the condition is satisfied, the algorithm is terminated; otherwise, it is continued.
6. We perform QRS detection in the selected source signal ($\widehat{z}^{[\ell]}_{v^{[\ell]}}(n)$), and the results are stored in set $\mathcal{R}^{[\ell]} = \left\{ r^{[\ell]}_i \,\middle|\, i = 1, 2, \cdots, N^{[\ell]}_r \right\}$ where $r^{[\ell]}_i$ denotes the location of the i-th complex, $N^{[\ell]}_r$ is the number of complexes detected.
7. Set $\mathcal{R}^{[\ell]}$ is compared with those obtained during the previous iterations ($\mathcal{R}^{[1]}, \cdots, \mathcal{R}^{[\ell-1]}$), and the first one with which it does not differ too much (when the total number of different QRS locations in both sets does not exceed the assumed allowable value – 60% of the previously detected complexes) replaces $\mathcal{R}^{[\ell]}$; the compared locations are regarded as coincident if they differ by less than 20 ms.
8. The chosen estimate undergoes filtering that is aimed to enhance the dominant ECG and to suppress the other components: $\widehat{z}'^{[\ell]}_{v^{[\ell]}}(n) = \mathrm{F}\{\widehat{z}^{[\ell]}_{v^{[\ell]}}(n)\}$; the operation can be accomplished with the use of projective [9] or adaptive impulse correlated filtering [10]; both types of filters require the knowledge of the QRS complexes locations – it is provided by set $\mathcal{R}^{[\ell]}$.
9. The filtered estimate of a source signal is projected back into the measurement space to reconstruct the corresponding components of the basic signals

$$\mathbf{r}^{[\ell]}(n) = \widehat{\mathbf{a}}^{[\ell]}_{v^{[\ell]}}\, \widehat{z}'^{[l]}_{v^{[\ell]}}(n), \tag{14}$$

   where $\widehat{\mathbf{a}}^{[\ell]}_{v^{[\ell]}}$ is the column of the mixing matrix, corresponding to the selected source signal: $\left(\widehat{z}'^{[\ell]}_{v^{[\ell]}}(n)\right)$.
10. The reconstructed components are subtracted from the basic signals to create their new form

$$\mathbf{x}^{[\ell]}(n) = \mathbf{x}^{[\ell-1]}(n) - \mathbf{r}^{[\ell]}(n). \tag{15}$$

11. If the iteration counter does not exceed the assumed maximal value, it is incremented ($\ell \leftarrow \ell + 1$) and the algorithm jumps to the second step of the next iteration; otherwise it terminates its operation.

The algorithm produces a new vector of source signals which were selected during the successive iterations: ${}_L\widehat{\mathbf{z}}(n) = \left[\widehat{z}^{[1]}_{v^{[1]}}(n), \cdots, \widehat{z}^{[L]}_{v^{[L]}}(n)\right]^\top$, where L is the number of iterations executed, a corresponding vector of the enhanced source signals: ${}_L\widehat{\mathbf{z}}'(n) = \left[\widehat{z}'^{[1]}_{v^{[1]}}(n), \cdots, \widehat{z}'^{[L]}_{v^{[L]}}(n)\right]^T$, and a new estimate of the mixing matrix: ${}_L\widehat{\mathbf{A}} = \left[\widehat{\mathbf{a}}^{[1]}_{v^{[1]}}, \cdots, \widehat{\mathbf{a}}^{[L]}_{v^{[L]}}\right]$. The numbers of the signals generated by the maternal or the fetal hearts, composing the corresponding source subspaces of: the maternal ECG ($\mathcal{F}_1$) and the ECG of the first ($\mathcal{F}_2$) or the second fetus ($\mathcal{F}_3$) are determined during execution of the 7th step of the successive iterations – comparison of the sets containing the results of QRS detection (it is assumed that the source signals corresponding to the same sets compose the same source subspaces). Consequently, on the basis of vector ${}_L\widehat{\mathbf{z}}'(n)$, we can decompose the measured signals into the components from different sources

$$\mathcal{F}_p x_i(n) = \sum_{k \in \mathcal{F}_p} {}_L\widehat{a}_{i,k}\, {}_L\widehat{z}'_k(n), \qquad i = 1, \cdots, K, \tag{16}$$

where p is the number of a source subspace.

In the algorithm described, we do not try to establish the origin of the selected source signals, i.e. we do not try to differentiate the maternal ECG from the fetal one. Consequently, we have to process those signals with the use of the methods that are effective in both cases. Thus the most difficult task of QRS detection was accomplished by the algorithm described in [23]. It is based on normalized matched filtering; to detect each new complex it takes into account its predicted localization. In our experiments the detector was very effective when fetal ECG signals were analyzed, and it allowed for almost error free detection of the maternal complexes.

In this study the filtering operation, performed in the 8th step of the algorithm, was accomplished with the use of projective or adaptive impulse correlated filtering. The resulting methods are denoted as SDSS-PF or SDSS-AF, respectively.

3. Numerical experiments

Two experiments were performed to assess the method performance in processing the signals of the fetal twins. In the first experiment, we analyzed the genuine twin pregnancy signals. They allowed us to make some visual appraisal of the decomposition results. However, to make some quantitative assessment of the method efficiency, a simulation experiment was also conducted.

3.1. Qualitative experiment. In this experiment we applied the method to process 4 maternal abdominal four-channel signals, recorded during twin pregnancy. Each signal was of 5 min length, stored with the sampling frequency of 500 Hz. We applied the SDSS-PF method and for the projective filter the embedding dimension $m = 50$ was used, and different dimensions of signal subspaces: $Q = 2$ near the QRS complexes and $Q = 1$ in other regions of the ECG beats ($Q = 2|1$). Before the method application, the processed signals were filtered to suppress the low frequency noise and the power-line interference (the first cut-off frequency of the filter pass-band was equal to 5 Hz). The filter described in [26] was applied for this purpose; more advanced nonlinear approach [27] will be used in future applications.

The method operation is illustrated in Figs. 2–8. As we can notice, the processed signal (Fig. 2A) is a complicated mixture of the bio-electrical components generated in the hearts of the mother and the fetal twins. The twins components are not recognizable, but we can distinguish the maternal ECG. It is of relatively high rate, exceeding 100 bpm. It should be noted that such a high maternal heart rate is not uncommon in twin pregnancies because they place increased demands on the maternal circulation [28, 29].

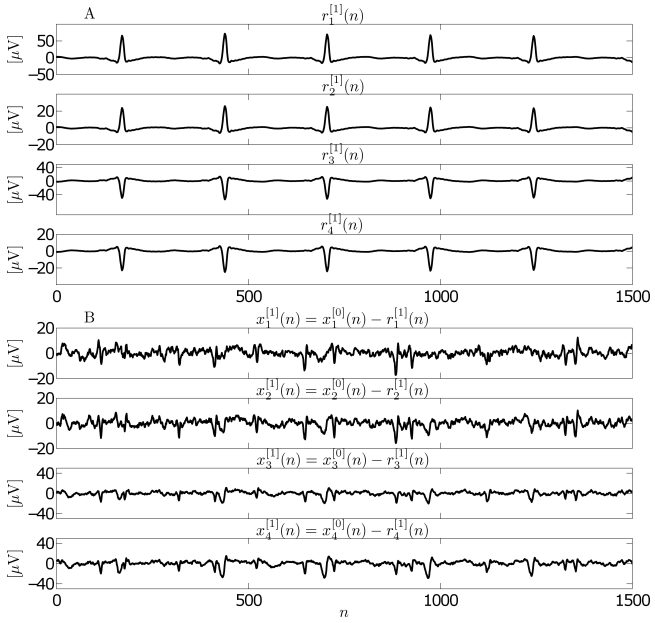

Fig. 3. Illustration of SDSS-PF operation: A) the components of the measured signals reconstructed on the basis of the source signal indicated by the arrow in the previous figure (after its projective filtering); B) the "basic" signals with the reduced number of independent components (obtained after the first iteration of the algorithm)

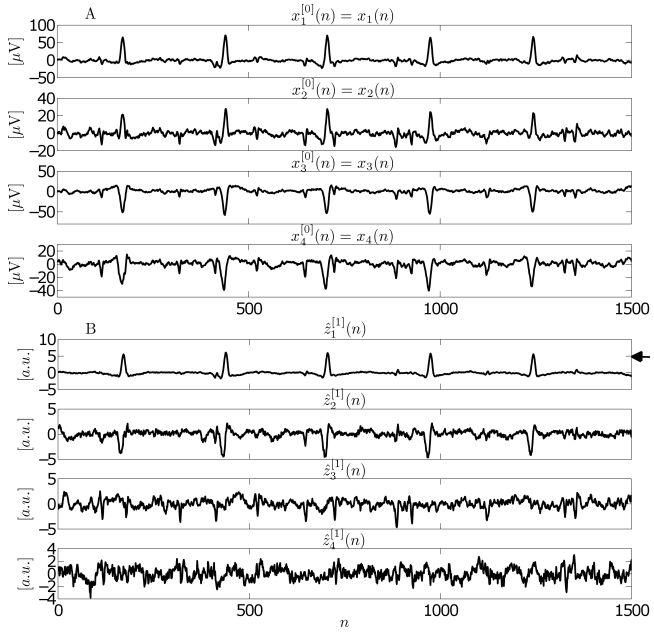

Fig. 2. Illustration of SDSS-PF operation: A) the measured signals $\mathbf{x}(n)$ which are the initial form of the "basic" signals: $\mathbf{x}^{[0]}(n)$; B) the source signals estimates calculated during the second step of the algorithm first iteration (the arrow indicates the estimate that achieved the largest value of the quality index); a.u. stands for arbitrary units

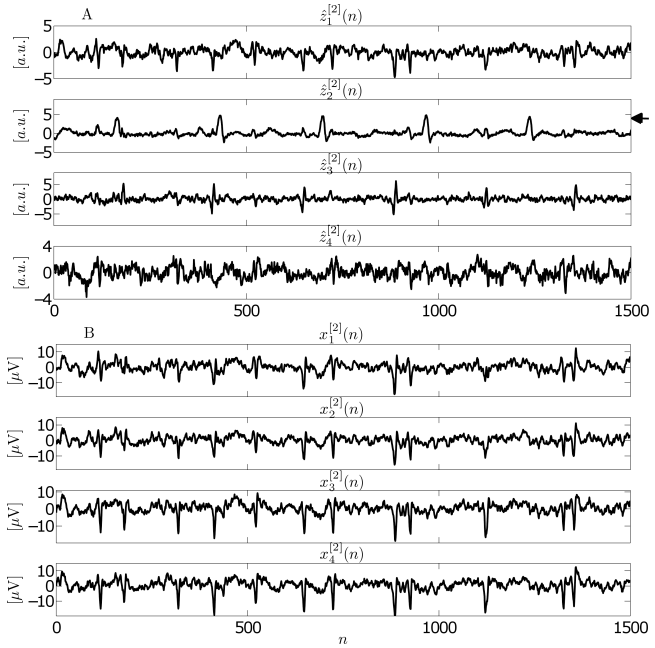

Fig. 4. Illustration of SDSS-PF operation: A) the source signals estimates calculated in the second step of the second iteration (the arrow indicates the estimate of the highest quality); B) the "basic" signals with the reduced number of independent components (obtained after the second iteration of the algorithm)

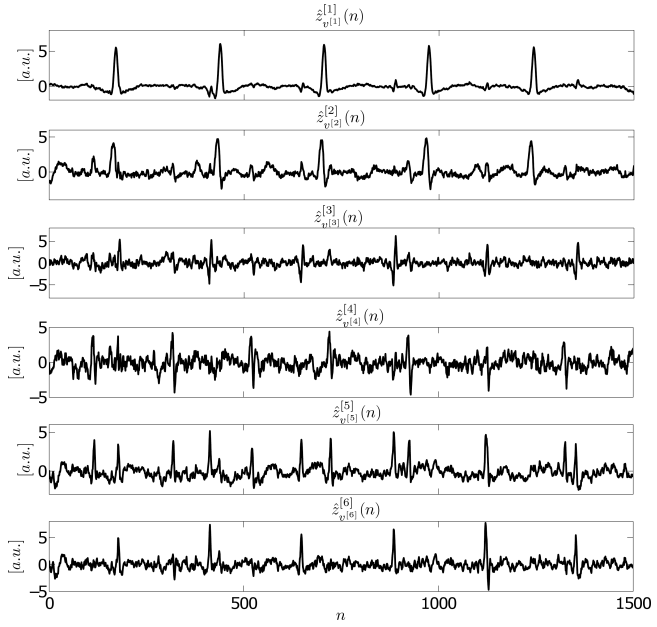

Fig. 5. The source signals estimates calculated during the successive iterations of the SDSS-PF method

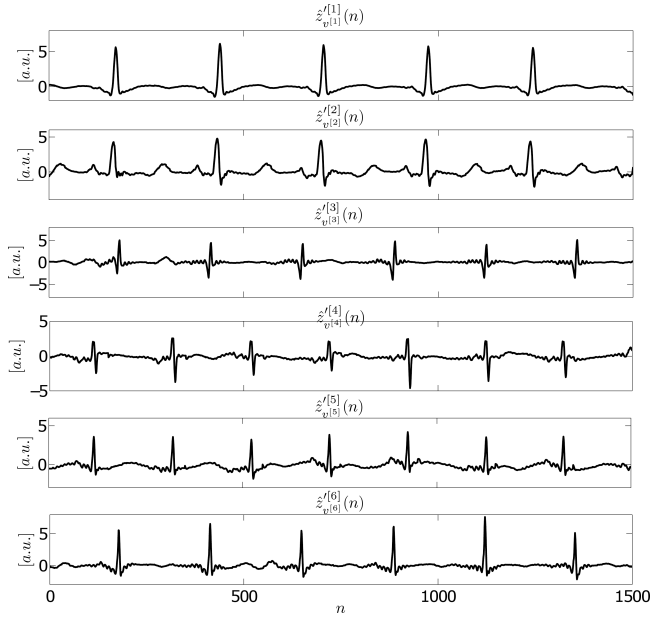

Fig. 6. Results of source subspaces determination by projective filtering and grouping of the source signals estimates. The maternal ECG source subspace: $\mathcal{F}_1 = \{1, 2\}$, contains the estimates $\widehat{z}'^{[1]}_{v^{[1]}}(n)$ and $\widehat{z}'^{[2]}_{v^{[2]}}(n)$; the ECG source subspace of the first fetus: $\mathcal{F}_2 = \{3, 6\}$, the estimates $\widehat{z}'^{[3]}_{v^{[3]}}(n)$ and $\widehat{z}'^{[6]}_{v^{[6]}}(n)$, and the subspace of the second fetus: $\mathcal{F}_3 = \{4, 5\}$, the estimates $\widehat{z}'^{[4]}_{v^{[4]}}(n)$ and $\widehat{z}'^{[5]}_{v^{[5]}}(n)$

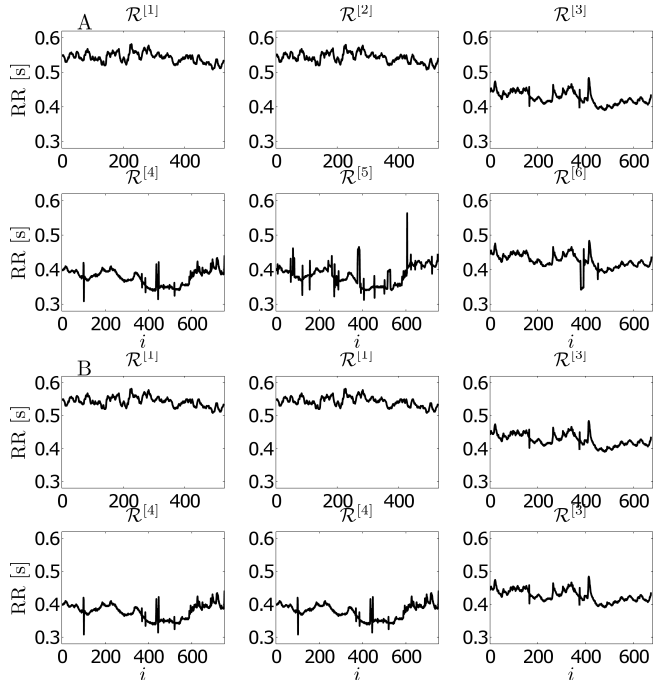

Fig. 7. Results of QRS complexes detection: A) obtained during the successive iterations of SDSS-PF algorithm, on the basis of the highest quality estimates of the source signals; B) chosen from the above in the 7th step of each iteration (as we can see $\mathcal{R}^{[2]}$ was replaced by $\mathcal{R}^{[1]}$, $\mathcal{R}^{[5]}$ by $\mathcal{R}^{[4]}$ and $\mathcal{R}^{[6]}$ by $\mathcal{R}^{[3]}$)

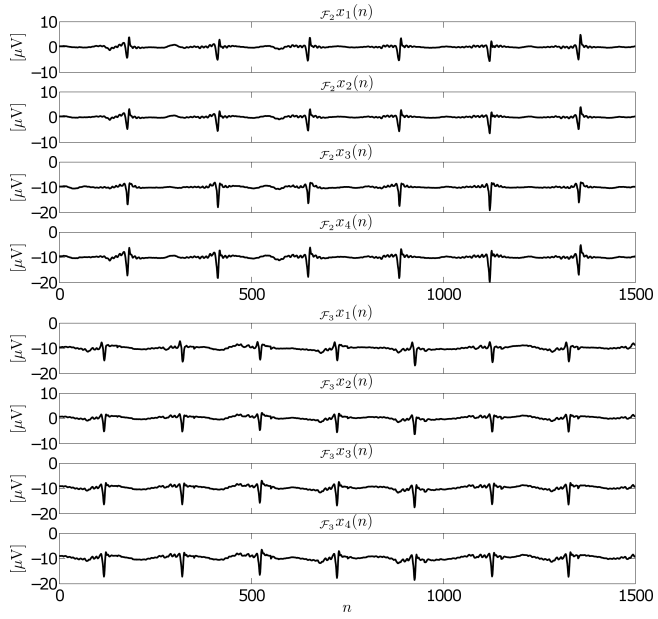

Fig. 8. Results of the twins ECGs reconstruction on the basis of their source subspaces: $\mathcal{F}_2$ and $\mathcal{F}_3$ from Fig. 6, respectively

In the second step of the first iteration of SDSS, applying the Jade algorithm, we obtained the source signals estimates presented in part B of Fig. 2. Clearly, the method was unable to separate the ECG signals involved. Only the estimate indicated by an arrow is dominated by a signal from one heart: it is the maternal one. For this estimate the largest value of the quality index ($QI^{[1]}_{\max}$) was achieved. Therefore according to the 8th step of SDSS, this estimate was enhanced by the projective filter. In the 9th step, the enhanced estimate was reprojected into the measurement space (14), and the corresponding components of the respective measured signals were reconstructed (Fig. 3A). Their subtraction (in the 10th step od SDSS) canceled one of the independent components of the recorded signal (compare Fig. 3B with Fig. 2A) and consequently resulted in significant suppression of the maternal ECG.

Execution of the second step of the second SDSS iteration allowed (Fig. 4) to separate not only the second maternal source signal but also the first fetal one ($\widehat{z}^{[2]}_3(n)$). However, the estimate of the maternal source signal obtained the highest value of the quality index. Therefore, it was this estimate that was processed in the second iteration and, as a result, the maternal ECG was almost completely removed from the basic signals (Fig. 4B).

In the example presented, the SDSS algorithm realized 6 iterations and, as a result, 6 source signals were selected (Fig. 5). On their basis the source subspaces were constructed (Fig. 6). As we can see in Fig. 5, during the first 4 iterations the source signals estimates corresponding to all interesting ECG components (of the mother and the both fetuses) were separated. However, in the fifth source signal $\left(\widehat{z}^{[5]}_{v^{[5]}}(n)\right)$ we can perceive the mixed components of the both fetal ECGs. Nonetheless, in the last estimate $\left(\widehat{z}^{[6]}_{v^{[6]}}(n)\right)$ the ECG of one fetus was again well separated. To gain an explanation of such SDSS operation, we should carefully analyze Figs. 6 and 7.

In Fig. 7A we presented the results of QRS complexes detection, performed in the sixth step of the successive iterations (sets $\mathcal{R}^{[\ell]}$, $\ell = 1, 2, \cdots, 6$). In part B of the figure, we can see the results of the comparison of these sets, performed in the 7th step of the algorithm. In this step, assuming that the detection performance can gradually decrease during the successive iterations, we were searching for similar results obtained during the previous iterations. Consequently, set $\mathcal{R}^{[2]}$ was replaced by $\mathcal{R}^{[1]}$, set $\mathcal{R}^{[5]}$ (with large number of detection errors, indeed) by $\mathcal{R}^{[4]}$ and similarly $\mathcal{R}^{[6]}$ by $\mathcal{R}^{[3]}$.

During the successive iterations, the chosen detection results were exploited by the projective filter enhancing the selected estimates of the source signals (from Fig. 5). The enhanced estimates are presented in Fig. 6. In most iterations the projective filter caused mostly suppression of noise, and this way more precise estimation of the selected source signals. However, in the 5th iteration it was this filter that allowed for suppression of one of the mixed signals of the twins. Thus, by filtering signal $\widehat{z}^{[5]}_{v^{[5]}}(n)$ from Fig. 5 we obtained signal $\widehat{z}'[5]_{v^{[5]}}(n)$ from Fig. 6, containing the separated FECG component of the second twin. Removing this signal from the basic ones allowed for a successful extraction of the last estimate of the fetal source signal ($\widehat{z}^{[6]}_{v^{[6]}}(n)$ from Fig. 5) during the last iteration. This way the SDSS-PF method created 3 two-dimensional source subspaces, corresponding to the ECGs of the mother and the both twins. Finally, as we can see in Fig. 8, the both fetal components of the respective channels were reconstructed.

Information on the results of the respective signals processing is given in Table 1: #FHR denotes the number of fetal heart rates determined, $|\mathcal{F}_k|$ – the dimension of the k-th source subspace created. As we can see, in three cases the proposed method allowed for successful analysis of the processed signals (the heart rates of both twin fetuses were determined: #FHR=2). It failed in one case only (#FHR=1), not being able to determine the heart rate of the second twin. However, in this case the amplitude of the second FECG was so small that visually no traces of its presence were perceivable (and, consequently, no subspace describing the ECG of the second twin could have been constructed: $|\mathcal{F}_3|\,0$). It should be emphasized that, apart from this single case, the SDSS method allowed us not only to detect the fetal heart rates, but also to determine the source subspaces and to reconstruct the fetal ECG signals of the both twins.

Table 1
Results of SDSS-PF in the genuine twin pregnancy signals: $\#FHR$ denotes the number of fetal heart rates determined, $|\mathcal{F}_k|$ is the dimension of the kth source subspace with 0 meaning that the subspace has not been constructed ($\mathcal{F}_1$ refers to the maternal whereas $\mathcal{F}_2$ and $\mathcal{F}_3$ to the fetal ECGs)

#signal	#FHR	$\lvert\mathcal{F}_1\rvert$	$\lvert\mathcal{F}_2\rvert$	$\lvert\mathcal{F}_3\rvert$
1	2	2	2	1
2	1	1	2	0
3	2	2	2	2
4	2	2	2	2

3.2. Quantitative experiment. Although possibility to determine a few source subspaces and then to reconstruct the ECG signals of the fetal twins seems to be rather useful, since it provides new information on the signals morphology, the basic goal that can be achieved with the developed method (SDSS) is determination of the heart rates of these fetuses. To investigate quantitatively the method performance in this application, we combined the signals recorded during single pregnancies to construct signals containing the components of 2 fetuses. To this end we used five records from the Physionet database of abdominal and direct fetal electrocardiogram [1, 30]. They are denoted as r01, r04, r07, r08 and r10. Each of them contains four-channel maternal abdominal traces, a simultaneously recorded direct fetal ECG and the reference locations of the fetal QRS complexes (the signals, originally stored with the sampling frequency of 1000 Hz, were decimated by a factor of 2).

We applied the SDSS-PF method (with $m = 50$, $Q = 2|1$ as in the previous paragraph) to each of these signals (the ma-

ternal abdominal ECG traces) and we constructed the source subspaces associated with the maternal and the fetal ECG. The maternal source subspaces were used to reconstruct and suppress the maternal components of the measured signals. This way we obtained the four-channel fetal ECGs with only negligible residuals of the MECG component but all other types of noise preserved. Then we combined the original signals with those with the MECG suppressed, obtaining $5 \cdot 4 = 20$ signals of the simulated twin pregnancy (with known locations of the fetal QRS complexes). The signals are denoted by pairs (k, i) where $k \in \{1, 2, \cdots, 5\}$ is the number of the original signal, i.e. the number of the maternal ECG and the ECG of the first fetus, and $i \in \{1, 2, \cdots, 5 | i \neq j\}$ is the number of the second FECG added.

On the basis of the source subspaces associated with the fetal ECGs, we obtained some information on the spatial distribution of these components. First, for each of the 5 original records, we reconstructed the fetal components of the measured signals. Then we estimated their covariance matrix and calculated the eigenvector $\mathbf{v}$ corresponding to the largest eigenvalue of this matrix. This eigenvector is the first principal direction of the fetal ECG in the measurement space.

Knowing the principal directions of the both fetal ECGs in the simulated signals, we calculated the modulus of the angle between them. Since the cosine of the angle between two normalized vectors is equal to their dot product, the angle itself can be calculated as the cosine inverse of the dot product

$$|\angle_{k,i}|[^\circ] = \frac{180^\circ}{\pi} \arccos \left| \mathbf{v}_k^\top \mathbf{v}_i \right|, \tag{17}$$

where k and i are the numbers of the first and the second FECG in the simulated twin pregnancy signal. This angle can provide us some measure of the spatial separability of the simulated twin electrocardiograms. For $|\angle_{k,i}| = 0$ (when the dot product is equal to one) the both fetal signals are projected in the same way into the respective leads and they cannot be spatially separated. On the other hand, for $|\angle_{k,i}| = 90^\circ$ (when the dot product is equal to zero) their separability is easiest.

It should be mentioned that this measure of separability can only be applied for signals whose spatial distribution is well defined by the first principal direction, with only a small dispersion into other directions, and it was the case in all single pregnancy FECG signals used.

Using the signals simulated, six different decomposition methods were investigated. They are as follows:

1. SDSS-PF.
2. SDSS-AF.
3. ICA-PF: independent component analysis combined with projective filtering. In this method, proposed in [31], we first apply ICA, then we select the source signals estimates dominated by the maternal ECG, we enhance these estimates with the use of the projective filter and similarly as in SDSS method, we reconstruct, subtract and this way suppress the MECG components. Then we apply ICA once more to separate the ECGs of the twins.
4. ICA-AF: independent component analysis combined with adaptive filtering. This method is analogous to the third one, with the adaptive impulse correlated filter (AICF) replacing the projective one.
5. PF-ICA: projective filtering combined with independent component analysis. This is the very basic concept. In this method projective filtering is applied to suppress the maternal ECG in the individual abdominal channels. Then we apply ICA to separate the ECGs of the twins.
6. AF-ICA: adaptive filtering combined with independent component analysis. This method is similar to the fifth one, with the adaptive impulse correlated filter replacing the projective one.

The ICA-PF, ICA-AF, PF-ICA and AF-ICA methods will be considered as the reference for SDSS in the further part of the study.

For all methods ICA weights were estimated on the basis of the 20-s interval of the processed signal, beginning after the run-up period of all filters applied. The methods using projective filtering were applied with different values of embedding dimension m, varied from 30 to 100 with the step of 10. The applied dimensions of local signal subspaces were larger near the QRS complexes and smaller in other parts of ECG beats. Three different possibilities were tested: $Q = 2|1$, $Q = 2|0$ and $Q = 1|0$. For the methods using adaptive impulse correlated filtering, different values of the correction factor were applied: $\mu \in \{0.001, 0.002, 0.005, 0.01, 0.02, 0.05, 0.1, 0.2\}$.

The methods were applied to process each of the constructed signals, and the results of QRS detection in the extracted FECG components were compared to the reference QRS locations (the compared locations were regarded as coincident if they differed by less than 20 ms). Consequently, for each signal we obtained the number of false negative $\#FN1$ and false positive $\#FP1$ detections referring to the ECG of the first fetus, and the corresponding numbers $\#FN2$ and $\#FP2$ referring to the second FECG (for all signals the detection results occurring in the beginning and ending intervals of 1 s were neglected, and since in the r10 record the direct FECG was lost between 187 and 191 s, and between 203 and 211 s of the trace, in these parts of the signal they were neglected as well).

The total number of the detection errors obtained for all test signals, divided by the number of fetal QRS complexes in these signals (25296) gives the average error rate. This error was used as a criterion for selection of the most favorable parameters of the investigated methods. The results obtained by the respective methods, when applied with the selected most favorable parameters, are given in Table 2 ($\#FN$ and $\#FP$ denote the total number of false negative and false positive detections, respectively). We can notice that the method proposed, applied both with projective and with adaptive impulse correlated filtering, is much more effective than the reference methods. For all methods, exchanging PF with AICF caused only minor changes of their performance.

Table 2
The overall accuracy (error rate) of fetal QRS complexes detection: #FN and #FP denote the total number of false negative and false positive detections (the total number of complexes was equal to 25296)

	error rate [%]	#FN	#FP
SDSS-PF	6.6	813	866
SDSS-AF	7.5	938	964
ICA-PF	36.3	4241	4946
ICA-AF	42.2	4896	5775
PF-ICA	38.0	4213	5402
AF-ICA	39.5	3977	6016

We calculated for how many signals the methods were able to determine successfully the heart rates of the both fetuses, for how many one FHR only, and for how many they failed completely (the numbers are denoted as $N2$, $N1$ and $N0$, respectively). Determination of a heart rate was regarded as successful if the error rate was lower than the assumed threshold value. Table 3 presents those numbers obtained for three different thresholds. They are similar to the results from Table 2. The SDSS+PF method appeared the most advantageous. When only a low error rate (10%) was regarded as acceptable, it managed to process successfully 16 of the 20 simulated signals. When 30% of errors were allowed, this number increased to 19, and for the threshold of 50%, the analysis of all signals was regarded as successful. The reference methods were able to analyze only about half of the simulated signals.

Table 3
Results of fetal heart rate determination: N2/N1/N0, in the 20 simulated test signals, obtained when different Error Rates (ER) were allowed. N2, N1 and N0 denote respectively the numbers of signals for which 2 or 1 or 0 FHRs were determined

	ER $< 10\%$	ER $< 30\%$	ER $< 50\%$
SDSS-PF	16/0/4	19/0/1	20/0/0
SDSS-AF	15/1/4	19/0/1	19/0/1
ICA-PF	8/8/4	10/9/1	12/7/1
ICA-AF	7/9/4	8/11/1	10/9/1
PF-ICA	7/9/4	10/9/1	11/8/1
AF-ICA	7/9/4	10/9/1	10/9/1

For the most effective method (SDSS+PF), we presented the detection results obtained for the individual test signals (Table 4). To make interpretation of these results easier, we also provided the values of the calculated angle between the respective pairs of the FECG components (modulus of the angle between the first principal directions of these signals in the measurement space). This simple index of the signals spatial separability was calculated according to (17). We can perceive that the very significant majority of errors was obtained for four signals only: (1,4), (4,1), (2,3) and (3,2). This can be explained by the very small angles between these pairs of FECGs. However, the angle was also rather small for all other combinations of the numbers $\{1, 2, 3, 4\}$. This means that $2 \cdot 3 \cdot 2 = 12$ signals were hardly tractable by ICA (after maternal ECG suppression, as in the reference methods). Among the simulated 20 signals, only all combinations with the FECG #5 are spatially easily separable. And, indeed, in Table 3 we can see that for the reference methods, relying mostly on the ICA decomposition, at most 8 signals were successfully analyzed with the detection error smaller than 10%. Fortunately, the features that can be exploited by SDSS are the FECG components amplitude and shape. The applied detection algorithm allows for a successful detection of QRS complexes in the mixed FECG signals if only they differ with respect to these features. Consequently, the dominant FECG can be enhanced by application of projective or adaptive filtering. Subtracting this component, which could not have been spatially separated, we allow for more efficient application of ICA in further iterations of the SDSS algorithm. This way the method proposed, exploiting not only the spatial features of the processed signals, managed to analyze successfully their majority, although in all cases the number of source signals was larger than the number of the measured ones. Thus it seems possible to perform diagnostic analysis of the fetal heart rates of the twins with the use of the methods applied in single pregnancy cases [32].

Table 4
Detection results of SDSS-PF for the respective simulated test signals: N_1 and N_2 denote the total numbers of QRS complexes of the first and the second twin; $\#FN1, \#FP1, \#FN2, \#FP2$ are the numbers of false negative and false positive detections of these complexes

signal(k,i)	N_1	N_2	#FN1	#FP1	#FN2	#FP2	$= \lvert\angle_{k,i}\rvert$ [°]
(1, 2)	639	627	3	4	12	12	14
(1, 3)	639	622	4	5	4	3	13
(1, 4)	639	646	88	82	83	89	3
(1, 5)	639	628	8	9	2	1	35
(2, 1)	627	639	12	13	5	5	14
(2, 3)	627	622	155	146	142	139	2
(2, 4)	627	646	6	6	3	4	13
(2, 5)	627	628	5	5	0	0	40
(3, 1)	622	639	7	7	6	6	13
(3, 2)	622	627	55	54	71	67	2
(3, 4)	622	646	2	2	3	6	12
(3, 5)	622	628	1	1	0	0	41
(4, 1)	646	639	45	45	60	60	3
(4, 2)	646	627	8	9	10	10	13
(4, 3)	646	622	2	4	3	2	12
(4, 5)	646	628	8	10	3	2	33
(5, 1)	628	639	0	0	0	1	35
(5, 2)	628	627	1	1	16	15	40
(5, 3)	628	622	0	0	8	7	41
(5, 4)	628	646	0	0	2	4	33

For comparison, in [7] the successful separation of the eight-channel twin ECGs was achieved with the use of ICA alone. It was a simulation experiment. The successful experiment on the genuine 12-channel signals was described in [33]. In the work [34], presenting the most comprehensive investigations of the issue, an opinion was formulated that analysis of 12-channel twin pregnancy signals allows in most cases for successful separation of the ECGs of the both fetuses.

4. Conclusions

The SDSS method combines independent component analysis with projective or adaptive filtering to overcome the intrinsic incapability of spatial methods to separate source signals when the number of the measured ones is significantly smaller. Such a combination of spatial and temporal filtering helped us to solve the problem of fetal electrocardiograms separation during twin pregnancy. The method proposed managed to separate the ECGs of the twins in the four-channel electric signals from the maternal abdomen. It enabled us not only to determine the fetal heart rates but also to reconstruct the fetal signals embedded in the maternal ECG and noise. To the best of our knowledge, for so small number of measured signal channels such reconstruction has not been performed by other researchers yet.

Acknowledgements. This research was supported by statutory funds (BK-2015) of the Institute of Electronics, Silesian University of Technology. The work was performed using the infrastructure supported by the POIG.02.03.01-24-099/13 grant: GeCONiI – Upper Silesian Center for Computational Science and Engineering.

REFERENCES

[1] J. Jezewski, A. Matonia, T. Kupka, D. Roj, and R. Czabanski, "Determination of the fetal heart rate from abdominal signals: evaluation of beat-to-beat accuracy in relation to the direct fetal electrocardiogram", *Biomedical Engineering/Biomedizinische Technik* 57 (5), 383–394 (2012).

[2] D.J. Jagannath and A.I. Selvakumar, "Issues and research on foetal electrocardiogram signal elicitation", *Biomedical Signal Processing and Control* 10 (1), 224–244 (2013).

[3] J.H. Nagel, "Progress in fetal monitoring by improved data acquisition", *IEEE Eng. Med. Biol. Mag.* 3 (3), 9–13 (1984).

[4] B. Widrow, J.R. Glover, J.M. McCool, J. Kaunitz, C.S. Williams, R.H. Hearn, J.R. Zeidler, E. Dong, and R.C. Goodlin, "Adaptive noise cancelling: principles and the applications", *Proc. IEEE* 63 (12), 1692–1716 (1975).

[5] P. Bergveld, A.J. Kölling, and J.H.J. Peuscher, "Real-time fetal ECG recording", *IEEE Trans. Biomed. Eng.* 33 (5), 505–509 (1986).

[6] D. Callaerts, B. De Moor, J. Vandewalle, and W. Sansen, "Comparison of SVD methods to extract the fetal electrocardiogram from cutaneous electrode signals", *Med. Biol. Eng. Comput.* 28 (3), 217–224 (1990).

[7] L. De Lathauwer, B. De Moor, and J. Vandewalle, "Fetal electrocardiogram extraction by blind source subspace separation", *IEEE Trans. Biomed. Eng.* 47 (5), 567–572 (2000).

[8] V. Zarzoso and A.K. Nandi, "Noninvasive fetal electrocardiogram extraction: blind separation versus adaptive noise cancellation", *IEEE Trans. Biomed. Eng.* 48 (1), 12–18 (2001).

[9] M. Kotas, "Projective filtering of time-aligned beats for foetal ECG extraction", *Bull. Pol. Ac.: Tech.* 55 (4), 331–339 (2007).

[10] P. Laguna, R. Jane, O. Meste, P.W. Poon, P. Caminal, H. Rix, and N.V. Thakor, "Adaptive filter for event-related bioelectric signals using an impulse correlated reference input: Comparison with signal averaging techniques", *IEEE Trans. Biomed. Eng.* 39 (10), 1032–1044 (1992).

[11] T. Schreiber and D.T. Kaplan, "Nonlinear noise reduction for electrocardiograms", *Chaos* 6 (1), 87–92 (1996).

[12] F. Takens, "Detecting strange attractors in turbulence, in: Lecture Notes in Mathematics", *Dynamical Systems and Turbulence* 898 (1), 366–381 (1981).

[13] I.T. Jollife, *Principal Component Analysis*, Springer, New York, 2002.

[14] J.M. Leski, "Robust weighted averaging", *IEEE Trans. Biomed. Eng.* 49 (8), 796–804 (2002).

[15] A. Momot, M. Momot, and J. Leski, "Bayesian and empirical Bayesian approach to weighted averaging of ECG signal", *Bull. Pol. Ac.: Tech.* 55 (4), 341–350 (2007).

[16] M. Kotas, "Robust projective filtering of time-warped ECG beats", *Computer Methods and Programs in Biomedicine* 92 (2), 161–172 (2008).

[17] R. Romo Vazquez, H. Velez-Perez, R. Ranta, V. Louis Dorr, D. Maquin, and L. Maillard, "Blind source separation, wavelet denoising and discriminant analysis for EEG artefacts and noise cancelling", *Biomedical Signal Processing and Control* 7 (4), 389–400 (2012).

[18] R.A. Salido Ruiz, R. Ranta and V. Louis-Dorr, "EEG montage analysis in the blind source separation framework", *Biomedical Signal Processing and Control* 6 (1), 77–84 (2011).

[19] M.A. Klados, C. Papadelis, C. Braun, and P.D. Bamidis, "REG-ICA: A hybrid methodology combining blind source separation and regression techniques for the rejection of ocular artifacts", *Biomedical Signal Processing and Control* 6 (3), 291–300 (2011).

[20] L. Albera, A. Kachenoura, P. Comon, A. Karfoul, F. Wendling, L. Senhadji, and I. Merlet, "ICA-based EEG denoising: a comparative analysis of fifteen methods", *Bull. Pol. Ac.: Tech.* 60 (3), 407–418 (2012).

[21] J.-F. Cardoso and A. Soulemiac, "Blind beamforming for non Gaussian signals", *IEE Proceedings-F* 140 (6), 362–370 (1993).

[22] M. Kotas, *Nonlinear Projective Filtering of ECG Signals*, Silesian University Press, Gliwice, 2011, (in Polish).

[23] M. Kotas, J. Jezewski, A. Matonia, and T. Kupka, "Towards noise immune detection of fetal QRS complexes", *Computer Methods and Programs in Biomedicine* 97 (3), 241–256 (2010).

[24] J. Cardoso, "Multidimensional independent component analysis", *Proc. 1998 IEEE Int. Conf. on Acoustics, Speech and Signal Processing, ICASSP* 4 (1), 1941–1944 (1998).

[25] M. Almeida, J. Bioucas-Dias, R. Vigario, and E. Oja, "A comparison of algorithms for separation of synchronous subspaces", *Bull. Pol. Ac.: Tech.* 60 (3), 455–460 (2012).

[26] J.A. Van Alste, W. Van Eck, and O.E. Herrmann, "ECG baseline wander reduction using linear phase filters", *Computers and Biomedical Research* 19 (5), 417–427 (1986).

[27] J.M. Leski and N. Henzel, "ECG baseline wander and powerline interference reduction using nonlinear filter bank", *Signal Processing* 85 (4), 781–793 (2005).

[28] S. Hunter and S.C. Robson, "Adaptation of the maternal heart in pregnancy", *British Heart J.* 68 (6), 540–543 (1992).

[29] M. Kuleva, A. Youssef, E. Maroni, E. Contro, G. Pilu, N. Rizzo, G. Pelusi, and T. Ghi, "Maternal cardiac function in normal twin pregnancy: a longitudinal study", *Ultrasound Obstet. Gynecol* 38 (5), 575–580 (2011).

[30] A.L. Goldberger, L.A. Amaral, L. Glass, J.M. Hausdorff, P.Ch. Ivanov, R.G. Mark, J.E. Mietus, G.B. Moody, C.-P. Peng, and H.E. Stanley, "PhysioBank, PhysioToolkit, and PhysioNet: components of a new research resource for complex physio-

logic signals", *Circulation* 101 (23), e215–e220 (2000).

[31] M. Kotas, "Combined application of independent component analysis and projective filtering to fetal ECG extraction", *Biocybernetics and Biomedical Engineering* 28 (1), 75–93 (2008).

[32] M. Jezewski, J. Wrobel, P. Labaj, J.M. Leski, N. Henzel, K. Horoba, and J. Jezewski, "Some practical remarks on neural networks approach to fetal cardiotocograms classification", *29th Annual Int. Conf. IEEE Engineering in Medicine and Biology Society, Lyon* 7, 5170–5173 (2007).

[33] P. Baxter, G. Spence, and J. McWhirter, "Blind signal separation on real data: tracking and implementation", *Proc. 6th Int. Symp. Independent Compon. Anal. Blind Signal Separ., Lecture Notes in Computer Science* 3889, 327–334 (2006).

[34] M.J. Taylor, M.J. Smith, M. Thomas, A.R. Green, F. Cheng, S. Oseku-Afful, L.Y. Wee, N.M. Fisk, and H.M. Gardiner, "Non-invasive fetal electrocardiography in singleton and multiple pregnancies", *Int. J. Obstetrics and Gynaecology* 110 (7), 668–678 (2003).